

# DYNAMIC APERTURE OPTIMIZATION USING GENETIC ALGORITHMS\*

C. Sun<sup>†</sup>, D. Robin, H. Nishimura, C. Steier and W. Wan, ALS, LBNL, CA 94720, U.S.A

## Abstract

Genetic Algorithm is successfully applied to optimize dynamic aperture of ALS storage ring lattices for future upgrades. It is demonstrated that the optimization using total diffusion rate as objective has a better performance than the one using dynamic aperture area. The linear and non-linear properties of the lattice are optimized simultaneously, and trade-offs are found among the small emittance, low-beta function and large dynamic aperture. These trade-offs can provide us a guideline to choose a candidate lattice for ALS future upgrades.

## INTRODUCTION

Optimization of dynamic aperture is a challenging aspect of storage ring lattice design. A large dynamic aperture is favorable for efficient injection and long beam lifetime. Several methods have been successfully applied by lattice designers to enlarge the dynamic aperture of storage ring. These methods include the resonance driving term minimization [1], brute force sextupole scan [2], and genetic optimization [3].

In this work, we will apply the genetic algorithms to optimize the dynamic aperture of ALS storage ring lattice for future upgrades. The genetic optimization is a method to find optimal solutions by mimicking the process of natural evolution, such as inheritance, mutation, selection and crossover. We demonstrate that the optimization using total diffusion rate as objective has a better performance than the one using dynamic aperture area. The linear and non-linear properties of the lattice are optimized simultaneously, and trade-offs are found among the small emittance, low beta function and large dynamic aperture. These trade-offs can provide us a guideline to choose a candidate lattice for ALS future upgrades.

## OPTIMIZATION OBJECTIVES

To optimize the dynamic aperture of a storage ring lattice using Genetic Algorithms (GA), first we need to properly choose quality factors, i.e., the optimization objectives. The most commonly used objective by ring designers is the dynamic aperture area. It is generally believed that the larger the aperture area the better the dynamic properties of the lattice is. However, the dynamic aperture area cannot give the detailed nonlinear behavior of particles, and the

resonance structures of the ring lattice can not be identified.

Frequency Map Analysis (FMA) can address these limitations. This technique has been introduced to study dynamics of particle accelerator for more than 15 years. Briefly speaking, FMA constructs a map between x-y configuration space and  $\nu_x$ - $\nu_y$  tune space by tracking particles with different initial coordinates for a period time (for example, 2N turns). For each test particle, the discrete trajectories are recorded at an observation location. Using the Numerical Analysis of Fundamental Frequencies (NAFF) algorithm [5], we can precisely calculate the tunes of this particle. As a stability index, the diffusion rate of particle trajectory is defined as follows

$$d = \log \left( \sqrt{\frac{(\nu_{x,1} - \nu_{x,2})^2 + (\nu_{y,1} - \nu_{y,2})^2}{N}} \right), \quad (1)$$

where  $\nu_{x,1}$  and  $\nu_{y,1}$  represent the horizontal and vertical tunes calculated for the first N turns tracking data;  $\nu_{x,2}$  and  $\nu_{y,2}$  represent the horizontal and vertical tunes calculated for the following N turns. Due to the logarithmic scale, the diffusion rate defined in Eq. (1) is always negative. A large negative number indicates that the diffusion is small and the particle trajectory is stable, while a small negative number indicates the diffusion is large and the particle motion is irregular.

Incorporating the diffusion rate to the dynamic aperture evaluation, we can obtain a powerful tool to study the nonlinear dynamic performance of a storage ring. For each test particle in x-y configuration space, not only its survival status is recorded, but also its diffusion rate is calculated. The total diffusion rate is then given by the summation of all the particle diffusion rates. Using total diffusion rate as an objective to optimize dynamic aperture of a lattice was first proposed in [6]. Instead of maximizing dynamic aperture area, if it is possible to minimize the total diffusion rate, the optimized lattice will have excellent dynamic performance.

## NONLINEAR OPTIMIZATION

In this section, we will apply the Non-dominated Sorting Genetic Algorithm II (NSGA-II) to optimize the dynamic aperture of the low-emittance lattices shown in Fig. 1 for ALS potential future upgrades. The details of this algorithm can be referred to [4]. The optimization parameters are sextupole strengths. At the current stage, the ALS storage ring lattice has two chromatic sextupole families (“SF” and “SD”) in arcs. However, after the baseline upgrade is finished, additional four harmonic sextupoles (“SHF”, “SHD”, “SHF1” and “SHD1”) will be installed in straight

\* Work supported by the Director Office of Science of the U.S. Department of Energy under Contract No. DE-AC02-05CH11231

<sup>†</sup> ccsun@lbl.gov

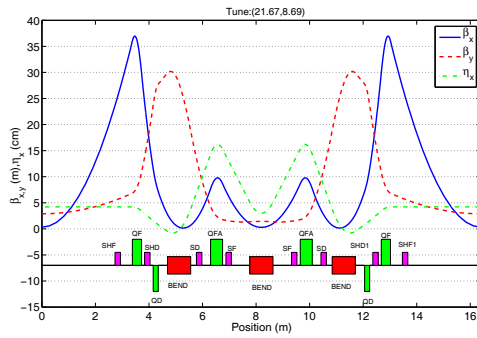
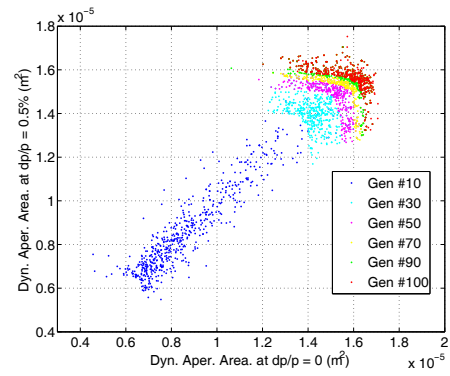


Figure 1: Layout of one sector of ALS ultimate upgrade lattice and its associated optics functions.

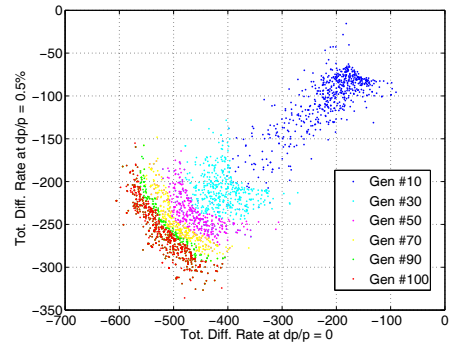
sections of each sector [7]. The arrangement of these chromatic and harmonic sextupole are shown in Fig. 1. The strengths of chromatic sextupoles are determined by the chromaticity fitting. Thus, in this optimization problem, there are four free parameters, i.e., the strengths of the harmonic sextupoles.

To compare the optimization performance, both the dynamic aperture area and total diffusion rate are used as optimization objectives. The accelerator modeling codes, such as Goemon [8] and Elegant [9], can be used for particle tracking and objective evaluations. Fig. 2 shows solutions at different generations in the objective spaces for the optimizations using (a) dynamic aperture area as objective and (b) total diffusion rate as objective. In either case, the objectives are calculated for both on- and off-momentum ( $dp/p = 0.5\%$ ) particles. The particles are tracked through the lattice with quadrupole strength and roll errors. The magnitude of these errors are 0.03% and 0.5 mrad, respectively. For the dynamic aperture area calculations, the 21-line search mode [9] is used and particle is tracked for 512 turns; the boundary of the aperture is clipped to avoid island before calculating the aperture area. For the total diffusion rate calculation, the particles are launched over non-uniform 21 by 21 grids in x-y space and tracked for 512 turns (The non-uniform grids in x-y space lead to an equal spacing in action space). For the surviving particles, the diffusion rates are calculated according to Eq. (1). If the particles are lost, the diffusion rates are assigned to a value which is slightly larger than the largest diffusion rate for surviving particles. In this problem, the number -3 is used. From Fig. 2, we can see that the solutions converge after 100 generations for either case, and an optimal solution front is obtained.

The Frequency Maps of example lattices from the solution fronts are shown in Fig. (3) for (a) optimization using aperture area as objective and (b) optimization using total diffusion rate as objective. In the figure, the diffusion rates of particle motions are represented by color. The blue color indicates that the particle orbit is stable, while the red color indicates the particle motion is chaotic. We can see that these two optimal lattices have almost the same aperture size. However, the lattice optimized using total diffusion



(a)



(b)

Figure 2: Solutions in the objective spaces at different generations for the lattice optimized using (a) dynamic aperture area as objective and (b) total diffusion rate as objective.

rate as objectives has a better dynamic performance than the lattice optimized using the aperture area, because in Fig. 3(b) there are less red color and some resonance structures also disappear. This demonstrates that the dynamic aperture optimization using total diffusion rate as objectives has a better performance than the optimization using dynamic aperture area as objectives.

## LINEAR AND NONLINEAR LATTICE OPTIMIZATION

In this section, we explore to optimize the linear and nonlinear properties of lattice simultaneously using NSGA-II. The lattice we are going to optimize is the same as the one used in previous Section. It has 12 superperiods with three quadrupole (“QF”, “QD” and “QFA”), two chromatic sextupole (“SF” and “SD”), and four harmonic sextupole (“SHF”, “SHD”, “SHF1” and “SHD1”) families. The three quadrupole strengths are used as parameters for the linear property optimizations, and four harmonic sextupoles are used for nonlinear property optimizations, and two chromatic sextupoles are used for chromaticity fittings. The objectives we want to optimize are two linear properties (horizontal beta function  $\beta_x$  at the center of straight and horizontal natural emittance  $\epsilon_x$ ), and one nonlinear property (the dynamic aperture area). The constraints are to ensure

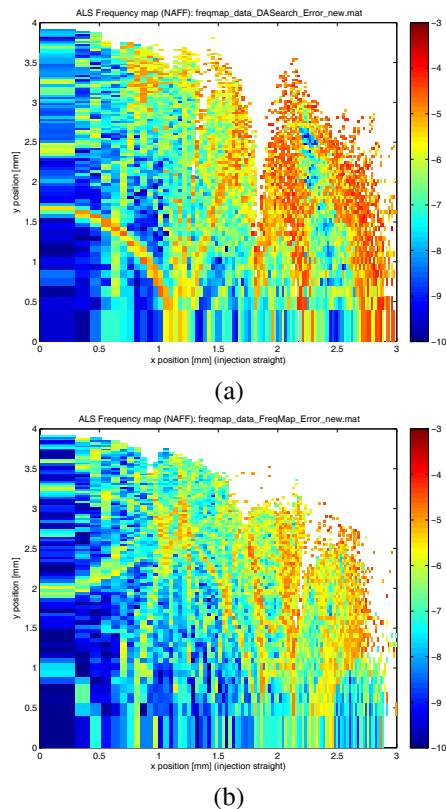


Figure 3: Dynamic aperture of lattice optimized using (a) dynamic aperture area as objective and (b) total diffusion rate as objectives. The diffusion rate of particle motions are color coded in the plot. The blue color represent particle is very stable, and red color present very chaotic.

the stability of the lattice, positive damping, and reasonable maximum Twiss and dispersion functions, and vertical phase advance.

The optimal solutions in the objective spaces are shown in Fig. 4. For this optimization problem, 20000 populations and 400 generations are used, and it take about 70 hours with 64 CPUs to reach these solution front using Lawrence cluster at Lawrence Berkeley National Laboratory [10]. In the figure, we can clearly see that there are trade-offs between small emittance ( $\epsilon_x$ ), large dynamic aperture and small horizontal beta function ( $\beta_x$ ). In previous section, the emittance of the lattice we try optimize is about 1.6 nm-rad. Fig. 4. shows that the dynamic aperture we can achieve for this lattice is about  $2 \times 10^{-5} \text{ m}^2$ . If we give up the emittance to 2.5 nm-rad, the dynamic aperture is almost doubled. These optimal solution fronts provide us guidance to choose a candidate lattice for ALS future upgrade.

## CONCLUSIONS

In this work, we have successfully applied Genetic Algorithms to optimize dynamic aperture of ALS upgrade lattices. It is demonstrated that the optimization using total

**Beam Dynamics and EM Fields**

**Dynamics 02: Nonlinear Dynamics**

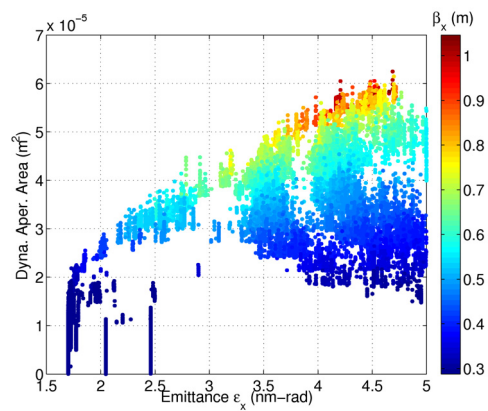


Figure 4: Linear and nonlinear optimizations of ALS lattice using NSGA-II. The lattice solutions are shown in the objective space, the horizontal emittance  $\epsilon_x$ , dynamic aperture area, and horizontal beta function  $\beta_x$  which is color coded.

diffusion rate as objective has a better performance than the one using dynamic aperture area. The linear and non-linear properties of the lattice are optimized simultaneously, and trade-offs are found among the small emittance, low beta function and large dynamic aperture. All the strategies and techniques presented in this paper are not limited to ALS lattice, and can also be applied to lattice of other facilities.

## ACKNOWLEDGMENTS

Authors would like to thank F. Sannibale and C. Papadopoulos at Lawrence Berkeley National Lab (LBL), L. Yang at Brookhaven National Lab (BNL) for fruitful discussions.

## REFERENCES

- [1] J. Bengtsson, SLS Note 9/97 (1997).
- [2] M. Borland, V. Sajaev, L. Emery, A. Xiao, Proceedings of PAC09, Vancouver, BC, Canada, TH6PFP062.
- [3] L. Emery, Proceedings of PAC05, Knoxville, Tennessee, pp. 2962-2964.
- [4] K. Deb, IEEE transactions on evolutionary computation, vol. 6, no. 2, pp.192-197 April 2002.
- [5] J. Laskar, *The Chaotic Motion Of The Solar System: A Numerical Estimate Of The Size Of The Chaotic Zones*, ICARUS, 88, 266-291 (1990).
- [6] C. Steier and W. Wan, Proceedings of IPAC'10, Kyoto, Japan, pp. 4746-4748.
- [7] C. Steier, *et. al.*, Proceedings of IPAC'10, Kyoto, Japan, pp. 2645-2647.
- [8] H. Nishimura, Proceedings of PAC01, Chicago, pp.3066-3068.
- [9] M. Borland, Advanced Photon Source LS-287, September 2000.
- [10] Laboratory Research Computing, <http://lrc.lbl.gov>.